

# Gain calculation of Semiconductor Optical Amplifier in Mach-Zehnder Interferometer Optical Switch

Indranil Jana<sup>1</sup>, Imran Hasan Choudhury<sup>2</sup>, Dilip Kumar Gayen<sup>2</sup>

<sup>1</sup>Department of Information Technology, College of Engg. and Management, Kolaghat

<sup>2</sup>Department of Computer Science, College of Engg. and Management, Kolaghat

CEMK, Midnapur (East), 721171, WB, India

jana.indranil@gmail.com, imzu.chou@gmail.com, dilipgayen@yahoo.co.in

**Abstract**—Proposed in this paper is a novel waveform scheme of modal gain of semiconductor optical amplifier (SOA) in Symmetric Mach-Zehnder Interferometer (SMZI). The effect of cross-phase modulation (XPM) and cross-gain modulation (XGM) in SOA and the interfering characteristics of MZI are combined to make the proposal simple, fast and integrable. Through numerical analysis and properly design of the parameters more than 20dB intensity contrast ratio of 100G/s RZ pseudorandom bit sequence can be achieved.

**Keywords**—SOA, SMZI, XPM, XGM, Contrast Ratio

## I. INTRODUCTION

Measuring the gain of SOA in SMZI in terms of waveform of short optical pulse is useful in many fields, such as optical fiber communication, fiber-optic sensor, laser spectroscopy, optical ranging, and many other related fields. All optical equivalent-time sampling technique has emerged in last few years. At the core of these techniques is an optical nonlinearity [1]. Compared to those sampler used fiber, grating and crystal, high-speed optical switch based on SOA have some advantages such as simple, stable, low cost, easy control and possibility of integration [2]. Another optical switch Terahertz Optical Asymmetric Demultiplexer (TOAD) needs high power control pulse to obtain good sampling contrast. Those drawbacks could be overcome by using Symmetric Mach-Zehnder Interferometer Optical Switch (SMIOS) as sampler. SMIOS only need femto-joule control pulse and achieve nearly ideal sampling windows [3]. In this switch, two SOAs are placed in each arm of MZI. When they are excited by control pulses which have some delay between them, the sampling windows appear. In this paper we analyze the gain of the SOAs and switching window. If the control and clock energies are properly selected so that the SOAs are heavily saturated and at the same time the switched-out pulses are not distorted, the metrics that define the quality of switching can be optimized for high gate performance at 10 Gb/s. The simulated result is shown using Matlab.

### A. Operation Principle and Block Diagram of SMIOS

Our study consists of a symmetrical MZI with one SOA located in the same relative position of each arm with the number of 3 dB couplers, as shown in Fig. 1 to calculate the gain and switching window of the SOA. The operation principle is based on the optically induced refractive index change within the SOA through appropriately synchronized

optical control pulse (CP) trains that alter the phase conditions of data signals in the interferometer, thus resulting in switching. Control and data signals, with orthogonal polarization, are fed into the switch via 3 dB couplers and co-propagate within the switch. In the absence of CPs, the data signals entering the switch via a coupler (C1) split into two equal intensity signals with 90° phase shift which propagate along the upper and lower arms of the interferometer, respectively. Couplers C2 and C3 are in the bar state for data signal therefore, introducing no additional phase shift  $\Delta\phi$  in the interferometer. With no CP present, both the ports will experience the same relative  $\Delta\phi$  during propagation and recombine at the output of C4 and the data signal to be switched to the cross port. With CPs present  $\Delta\phi$  is introduced between the two arms of the interferometer, thus causing the data signals to be switched to the bar port. To achieve a complete switching at the output port, signal A enters the interferometer via C2 just before the target data signal. The CP will then saturate SOA1, thus changing its gain as well as its phase characteristics. When the data signal enters the interferometer following the CP1, it will experience a different  $\Delta\phi$  (i.e.  $\pi$ ) in the upper arm relative to the lower arm and the data signal emerges from the bar port. No signal emerges from cross port. Introducing the second CP2, delayed by  $\Delta t$  with respect to CP1, just after the data signal, into the interferometer via C3 will saturate SOA2, thus resulting in the same  $\Delta\phi$  as in the upper arm, thereby resetting the switch. Therefore, with this mechanism the SMZ switch-on-and-off time is controlled by fast optical excitation process which overcomes the slow relaxation time. Note that  $\Delta t$  determines the SMZ nominal width of the switching window (SW).

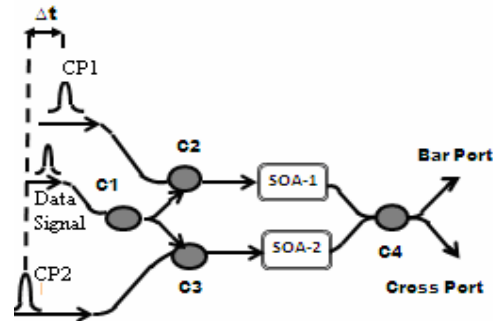


Fig 1: SMIOS block diagram.

### B. Operation Principle and Block Diagram of SOA

The most widely investigated active nonlinear optical component is the semiconductor optical amplifier (SOA). The main advantage of the SOA as compared to passive structures, e.g., optical fibers, is its compactness due to a resonant enhancement of the nonlinear optical effects. In this paper we calculate the gain variance of the SOA with respect to time. We also calculate switching window of the SOA. SOAs have attracted much attention for all optical switching applications, due to their high nonlinearity. In this section the basic properties of SOAs will be discussed, mainly with respect to their use in all-optical switching configurations. Fig. 2 shows schematically the typical structure of an SOA with input and output fibers. In this basic SOA configuration, light is coupled into the amplifier via one of the facets. Then it passes the active region once (in a single pass) before the light is coupled into the output fiber at the opposite side of the SOA. An efficient fiber-chip coupling can be achieved by use of a tapered fiber. Here, the taper acts as a micro-lens, which focuses the light onto the active region on the SOA facet. Typical values for the optical losses associated with the fiber-chip coupling are about 3 dB per facet.

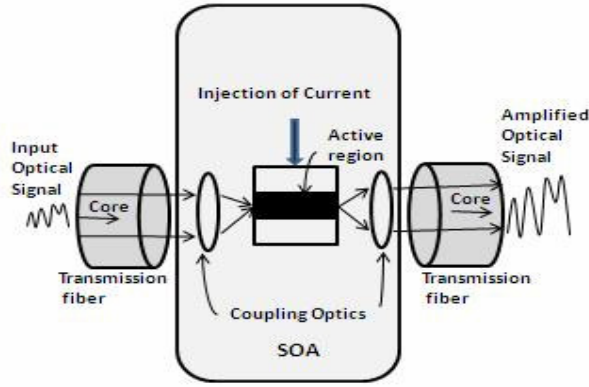


Fig. 2. Schematic of an Active region (e.g. InGaAsP/InP) in SOA device with fiber coupling.

The antireflection coating comprises multiple layers to achieve wide-band low facet reflectivity. The structure of the active region can be either bulk, multi-quantum well (MQW) or quantum-dot (QD). An MQW-SOA has generally a larger gain bandwidth and offers a higher degree of freedom with respect to the device design. The QD-SOA is of great interest because of its unique optoelectronic properties [4, 5].

### C. Basic Properties

The active semiconductor region of an SOA has a band structure as schematically depicted in Fig. 3. It is electrically pumped with carriers by the injection current. This results in population inversion between the conduction band and the valence band [6]. A light signal with frequency  $\omega$ , injected to the active region, is amplified by stimulated emission, if the photon energy  $\hbar\omega > E_g$ , where  $E_g$  is the band gap energy between valence band and conduction band and  $\hbar\omega < \Delta E_F = E_{Fc} - E_{Fv}$  between the quasi-Fermi levels  $E_{Fc}$  and  $E_{Fv}$  of the conduction band and valence band, respectively. The medium is transparent for photons with an

energy below the band gap ( $\hbar\omega < E_g$ ). The quasi-Fermi levels depend on the current-dependent population inversion. The band gap,  $E_g$  refers to the energy difference between the top of the valence band and the bottom of the conduction band in semiconductors. This is equivalent to the energy required to free an outer shell electron from its orbit about the nucleus to become a mobile charge carrier. A Quasi Fermi level describes the population of each type of charge carrier (electrons and holes) in a semiconductor separately when their populations are displaced from equilibrium which is caused by the application of an external electric potential, which injects electrons and holes. This increases the density of both electrons and holes above their equilibrium values.

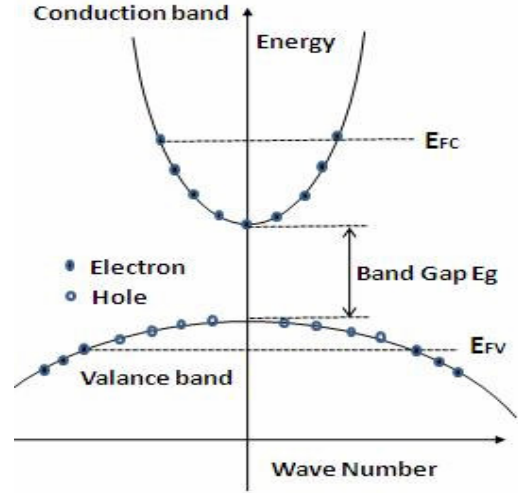


Fig. 3 Band structure of a direct band-gap semiconductor in quasi-equilibrium.

### D. Model Formulation

For simplicity, we neglect the loss and the amplified spontaneous emission (ASE) noise in SOA. Moreover, the power of the control data is assumed to be much larger than that of the probe pulses, thus the SOA dynamic gain can be regarded to be controlled only by the control-signals approximately. Considering the carrier pulsation effect and nonlinear gain compression effect of SOA induced by carrier heating and spectral hole burning. Here we consider Gaussian pulse as control signal, which is shown as

$$P_{in}(t) = \frac{U_{in}}{\tau_0 \sqrt{\pi}} \exp\left(-\frac{t^2}{\tau_0^2}\right)$$

Where,  $U_{in}$  is the incoming pulse energy,  $\tau_0$  is the full width at half maximum (FWHM). When a control pulse is injected into the SMZI, it saturates the SOA and changes its index of refraction. The dynamic gain  $g_1(t)$  and  $g_2(t)$  of SOA1 and SOA2 can be formulated as [7]

$$\begin{aligned} \frac{dh_1(t)}{dt} &= \frac{1}{1 + \varepsilon \exp[h_1(t)]P_1(t)} * \left\{ \frac{h_0 - h_1(t)}{\tau_c} \right. \\ &\quad \left. - \varepsilon [\exp[h_1(t)] - 1] \frac{dP_1(t)}{dt} - \right. \\ &\quad \left. [\exp[h_1(t) - 1]P_1(t) \left( \frac{\varepsilon}{\tau_c} + \frac{1}{E_{sat}} \right)] \right\} \dots (1) \\ \frac{dh_2(t)}{dt} &= \frac{1}{1 + \varepsilon \exp[h_2(t)]P_2(t)} * \left\{ \frac{h_0 - h_2(t)}{\tau_c} \right. \\ &\quad \left. - \varepsilon [\exp[h_2(t)] - 1] \frac{dP_2(t)}{dt} - \right. \\ &\quad \left. [\exp[h_2(t) - 1]P_2(t) \left( \frac{\varepsilon}{\tau_c} + \frac{1}{E_{sat}} \right)] \right\} \dots (2) \\ g_i(t) &= \exp[h_i(t)], i = 1, 2 \dots (3) \end{aligned}$$

Where  $P_1(t)$  and  $P_2(t)$  are the power of control signal at port 1 and port 2,  $\varepsilon$ ,  $h_0$ ,  $\tau_c$ , and  $E_{sat}$ , are the nonlinear gain compression factor, the small signal gain, the carrier lifetime, and the saturation energy of SOA, respectively. Taking the length effect of SOA [8] into accounts, the function of  $G_i(t)$  and  $h_i(t)$  can be deduced approximately as follows:

$$G_i(t) = \exp \left[ \frac{1}{L} \int_{-L/2}^{L/2} h_i(t - 2z/v_{SOA}) dz \right] \dots (4)$$

$i = 1, 2$

where  $L$  is the SOA length,  $v_{SOA} = c/n_{SOA}$  is the signal velocity in SOA, and  $n_{SOA}$  corresponds to the SOA refractive index. Consequently we can calculate the signal power at the output ports of the SMIOS from the calculated gain. The signal powers at the output of the SMZ are given as:

$$P_{out,1}(t) = 0.25P_{in}(t)[G_1(t) + G_2(t) - 2\sqrt{G_1(t)G_2(t)}\cos(\Delta\phi)] \dots (5)$$

$$P_{out,2}(t) = 0.25P_{in}(t)[G_1(t) + G_2(t) + 2\sqrt{G_1(t)G_2(t)}\cos(\Delta\phi)] \dots (6)$$

Where,  $\Delta\phi = -0.5\alpha_{LEF} \ln(G_1(t)/G_2(t))$ .

$\alpha_{LEF}$  is the Linewidth enhancement factor,  $G_1$  and  $G_2$  are the temporal gain profiles of the SOA1 and SOA2, respectively. The switching window of the proposed circuit can be expressed as

$$SW = 0.25[G_1(t) - G_2(t) + 2\sqrt{G_1(t)G_2(t)}\cos(\Delta\phi)] \dots (7)$$

According to (7), the SMZ switch can provide an additional gain to the target signal, thus ensuring that the SW gain  $> 1$ . To solve (7) one needs to know precise value of  $\alpha_{LEF}$  and the gain profiles of the data signals at the output of the SOA1 and SOA2, respectively. We try to simulate gain profile of SOA1 and SOA2.

## II. NUMERICAL SIMULATION AND RESULT

We investigate the dynamics gain characteristics of the SOA through numerical simulation. In modeling, the SOA parameters are given in Table 1 as following:

TABLE 1 :PARAMETER LIST

Parameters	Value
Nonlinear gain Compression Factor, $\varepsilon$	$0.4 \text{ w}^{-1}$
Line width enhancement factor, $\alpha$	5
Small signal gain, $h_0$	20dB
Carrier life time, $\tau_c$	300 ps
Saturation power, $P_{sat}$	25 dBm
SOA length, $L$	100 $\mu\text{m}$
SOA refractive index, $n_{SOA}$	3.62
Wave length of control signal, $\lambda_c$	1.53 mm
Wave length of data signal, $\lambda_p$	1.53 mm
Pulse width of the control signal, $T_{CP}$	5 ps
Pulse width of the data signal, $T_p$	5 ps
Power of the control signal, $P_c$	10 dBm
Power of the data signal, $P_p$	0.8 dBm
Saturation energy of the SOA, $E_{sat}$	1000 Fj
Control pulse energy, $E_{cp}$	100 Fj
Gain recovery, $\tau_e$	50 ms

Due to the superior transmission properties of RZ format compared to NRZ [9], both the control-signals and the probe pulses are RZ PRBS with 30 dB extinction ratio in analysis.

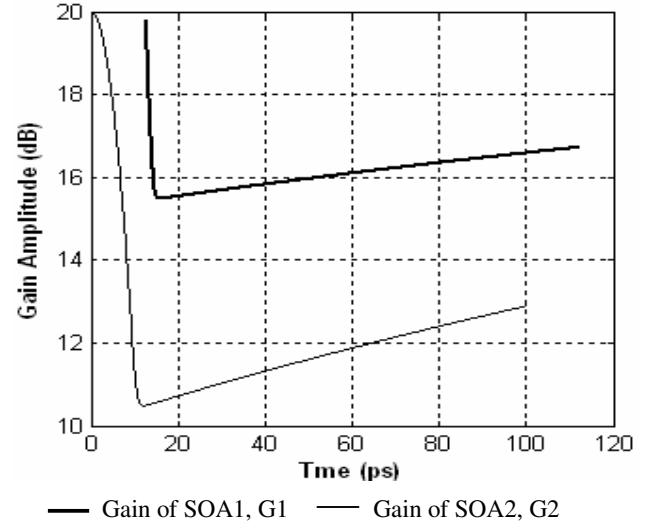


Fig. 4a. Gain Amplitude of SOA1 and SOA2

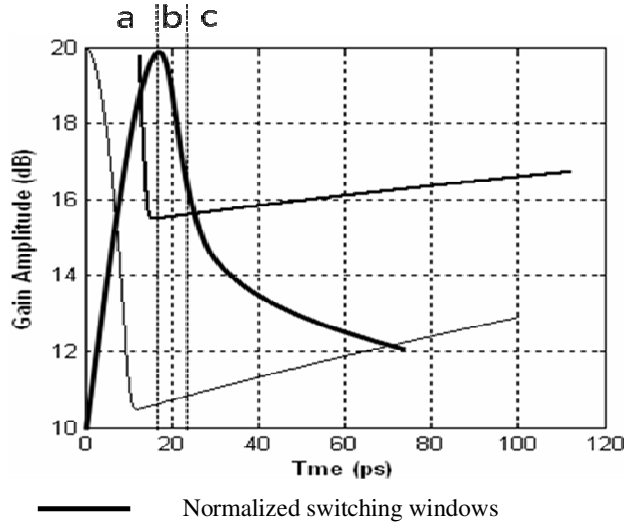


Fig. 4b. Gain Amplitude of SOA1 and SOA2 and normalized switching window

Fig. 4 describes the gain amplitude of SOA1 and SOA2 of the proposed SMIOS. Here small signal gain,  $h_0$  is 20dB.  $G_1$  and  $G_2$  describe the gain dynamics experienced by the data pulses in SOA1 and SOA2 and the symmetrical normalized SW denotes the normalized switching window interfered by the MZI. We calculate the gain  $G_1$  of SOA1 and the gain  $G_2$  of SOA2 with respect to time. The simulated form of the gain  $G_1$  and  $G_2$  is shown Fig 4a. Accordingly we calculate the normalized SW gain and the simulated waveform is shown in Fig. 4b. Note that  $\Delta t$  determines the SMZ nominal width of the SW. The gain dynamics of SOA1 and SOA2 can be divided into three periods, namely, the sharply-falling period (region a), the fast recovering period (region b) and the slow recovering period (region c), which is determined by the nonlinear gain compression effect. We note that the switching window opens when the SOA gain sharply falls and close laggardly along with the gain recovering. In view of it, we can draw a conclusion that the switching window and the dynamic gain of SOA are synchronous completely. After the short optical pulse has saturated the SOA according to following equation:

$$G(t) = \frac{1}{1 - (1 - \frac{1}{h_0}) \exp\left(-\frac{E_{cp}(t)}{E_{sat}}\right)} \quad (8)$$

Where  $E_{sat}$  is the saturation energy of the SOA,  $E_{cp}$  is the control pulse energy.

The gain recovers due to injection of carriers by the corresponding injection current. Assuming the general case of a pulse stream entering the SOA with a period less than its gain recovery time, the SOA gain does not have the time to fully recover to the small signal value but instead to a smaller initial gain. The gain approaches asymptotically the value as while at time it has reached saturation with gain. With these conditions, the SOA gain recovers due to injection of carriers can be obtained from the gain recovery formula:

$$G(t) = h_0 \left( \frac{G(t)}{h_0} \right) \exp\left(-\frac{(t-t_s)}{\tau_e}\right) \quad (9)$$

Where  $\tau_e$  the gain recovery is time and  $t_s$  is the saturation time of SOA. As a result, the two counter-propagation data signal will experience a differential gain saturation profiles i.e.  $G_1 \neq G_2$ . Therefore they recombine at the input coupler, and then  $\Delta\phi \approx \pi$  the data will exit from the output port 1. We calculate the value of  $G_1=16.7208$  dB and value of  $G_2=12.8903$  dB after gain recovery which is also evident from the Fig. 4a. We also calculate switching window 1.5610 dB, which is also evident from Fig 4b. An additional requirement for a pulse to be fully transmitted is that its width  $\sigma$  must be as short as possible and ideally less than the switching window.

### III. CONCLUSION

This paper addressed the semiconductor optical amplifier (SOA). The main focus was the application of SOAs for a TDM bit rate of 160 Gbit/s and above, because electrical signal processing is already available at a time division multiplexing bit rate up to 80 Gbit/s today. Accurate gain calculation is necessary to generate proper power in the output port. Next we will try to calculate bit error rate and contrast ratio of the SOA assisted MZI. The nonuniformity of the output signals can be improved through modulating the saturation power and the carrier lifetime of SOA.

### IV. REFERENCES

- [1] M. Westlund, P. Andrekson, H. Sunnerud, et al. High-Performance Optical-Fiber-Nonlinearity-Based Optical Waveform Monitoring. IEEE Journal of Lightwave Technology, 2005, 23(6):2012-2022
- [2] L. A. Jiang, E. P. Ippen, U. Feiste, et al. Sampling Pulse with Semiconductor Optical Amplifiers. IEEE Journal of Quantum Electronics, 2001, 37(1):118-126
- [3] Y. Zhao, P. Ye, Switching characteristic of semiconductor optical amplifier based demultiplexer with symmetric Mach-Zehnder interferometer configuration, Acta Opt. Sinica 22 (1) (2002) 99-106.
- [4] A. A. Ukhanov, A. Stintz, P. G. Eliseev, and K. J. Malloy, Comparison of the carrier induced refractive index, gain, and linewidth enhancement factor in quantum dot and quantum well lasers. Appl. Phys. Lett., 84 (7), 1058-1060 (2004).
- [5] T. Akiyama, K. Kawaguchi, M. Sugawara, H. Sudo, M. Ekawa, H. Ebe, A. Kuramata, K. Otsubo, K. Morito, and Y. Arakawa, "A semiconductor optical amplifier with an extremely high penalty-free output power of 20 dBm achieved with quantum dots, in Proc. 29th
- [6] Colja Schubert, Reinhold Ludwig, and Hans-Georg Weber, High-speed optical signal processing using semiconductor optical amplifiers. J. Opt. Fiber Commun. Rep. 2, 171-208 (2004) © 2004 Springer Science + Business Media Inc.
- [7] C. Xie, P. Ye, Analysis of all-optical demultiplexer used a semiconductor optical amplifier, Acta Photon. Sinica 27 (6) (1998) 159-166.
- [8] D. Breuer, et al., Comparison of NRZ and RZ modulation format for 40 Gbit/s TDM standard-fiber systems, in: Proc. ECOC'96, 1996, paper TuD3.3.
- [9] M. Young, The Technical Writer's Handbook. Mill Valley, CA: University Science, 1989.